

## Sb-mediated Ge growth on singular and vicinal Si(001) surfaces: A surface optical characterization study

J. R. Power,\* K. Hinrichs,† S. Peters, K. Haberland, N. Esser, and W. Richter

*Institut für Festkörperphysik, Technische Universität Berlin, PN6-1, Hardenbergstrasse 36, D-10623 Berlin, Germany*

(Received 10 November 1999; revised manuscript received 5 April 2000)

In this work, we apply Raman spectroscopy (RS) and spectroscopic ellipsometry (SE) to surfactant mediated growth (SMG) of Ge on Si(001) surfaces. Under molecular-beam epitaxy conditions, a growth temperature of 400 °C and in the absence of a predeposited surfactant (Sb) monolayer, we show that SE can be used to determine the Stranski-Krastanov critical thickness for island formation. In the presence of a predeposited Sb monolayer, SE predicts that layer-by-layer growth is possible up to a Ge coverage of 20 monolayers (MLs). However, no evidence of relaxation through dislocation formation, known to exist in this coverage regime, could be detected. With RS, we present one of the first studies of Sb mediated growth on a *vicinal* Si(001) substrate. Two Sb surface related phonon peaks are identified, one associated with Sb dimers bonded to the Si(001) substrate ( $130.5\text{ cm}^{-1}$ ), the other with Sb dimers on the grown Ge epilayer ( $141\text{ cm}^{-1}$ ). The former disappears and the latter appears gradually with increased Ge coverage up to 3.5 MLs. This indicates that surfactant exchange occurs differently on *vicinal* Si(001) than on *singular* Si(001), where exchange has been shown to be complete by deposition of between 0.5–1.0 monolayer (ML). To explain this difference, step bunching must occur during the initial stages of growth on *vicinal* Si(001), leading to areas of preferred growth on the surface. At a higher Ge coverage of 20 MLs, theoretical predictions of the Raman shift for a strained pseudomorphically grown Ge layer show good agreement with the Raman data presented. This demonstrates that even at 20 ML coverage, some areas of unrelaxed Ge must still exist, pointing to inhomogeneities within the Ge epilayer, as predicted by our model for SMG on a step bunched Si(001) substrate.

### I. INTRODUCTION

The layer-by-layer growth of Ge on Si(001) surfaces to thicknesses beyond those envisaged on the basis of interface free energies and lattice strain arguments can be promoted by exposing the Si substrate to small quantities of one of the group V elements, As, Sb, or Bi prior to growth.<sup>1–5</sup> In the absence of these group V elements, known as surfactants for the way they behave here, layer-by-layer growth of Ge on Si(001) is only possible up to approximately 3–6 monolayers (MLs).<sup>6–8</sup> In the 3–6 ML coverage region, two-dimensional (2D) islands start to form to alleviate the strain caused by the 4.2% lattice mismatch between both materials.<sup>9</sup> In the presence of a surfactant, strained layer-by-layer growth can be extended up to a critical thickness of 11–12 MLs, where dislocations form resulting in relaxation within the Ge layer.<sup>4,10,11</sup> However, all this work has been predominantly carried out on flat or *singular* Si(001) surfaces. By comparison, few studies detailing the initial stages of Ge growth on the stepped or *vicinal* Si(001) surface have appeared.<sup>12–14</sup> These studies, carried out solely on the bare surface without a surfactant, indicate that the growth of Ge on *vicinal* Si(001) leads to step bunching.<sup>13,14</sup>

For this system, surfactants work by limiting the diffusion of impinging Ge atoms so that no island is supplied with diffusing Ge necessary for its growth.<sup>15–17</sup> Thermodynamically, the free energy of this surface, where each Ge adatom contains dangling bonds can be reduced if Sb exchanges with Ge, producing Sb dimers on the surface which contain two unreactive lone pairs.<sup>2,15–17</sup> Microscopic models concerning the mechanism of surfactant exchange have been reported.

Recent work all points to the initial incorporation of Ge as dimers between intact and unperturbed Sb dimer rows, a process which must saturate at a Ge coverage of 0.5 ML. Once a second Ge dimer impinges upon the surface above this coverage, the Sb-Sb dimer bond is weakened and Sb dimer exchange is initiated.<sup>18</sup> Despite the large body of work concerning surfactant growth on the *singular* surface, by comparison, no significant experimental study exists yet that comprehensively explains surfactant mediated Ge growth on *vicinal* Si(001), although some theoretical work has appeared.<sup>19</sup> We report experimental data showing that changes in step structure must occur during the initial stages of surfactant mediated growth (SMG) on *vicinal* Si(001).

We apply the surface optical probe techniques, spectroscopic ellipsometry (SE) and Raman spectroscopy (RS), to this growth system. We take advantage of the large penetration depth of optical radiation to simultaneously obtain information concerning the buried Ge/Si(001) interface as well as the growing surface. Optical probe techniques have been shown recently to be very sensitive to changes in surface structure and stoichiometry and have the potential of providing microscopic information not only for surfaces in vacuum but also for surfaces under atmospheric conditions and even in liquids.<sup>20,21</sup> It will be shown that SE, which has been widely used in the past to determine properties such as film thickness, surface reconstruction change,<sup>22</sup> and surface roughness,<sup>22,23</sup> can also be used to distinguish changes in growth mode, for example, from layer-by-layer to island growth. Under the conditions used, we show that layer-by-layer growth in the absence of an Sb surfactant layer is limited to approximately 5 MLs. In the presence of an Sb layer, although layer-by-layer growth appears possible up to at

least 20 MLs, it is well known that relaxation through dislocation formation occurs in the region of 11–12 MLs. Hence SE here shows insensitivity to the formation of dislocations.

Using RS, interesting information concerning SMG from *vicinal* Si(001) is obtained. We identify two surface/interface features, one at  $130.5\text{ cm}^{-1}$  which we associate with Sb dimers on the Si(001) substrate and one at  $141\text{ cm}^{-1}$  which is related to Sb dimers on the grown Ge epilayer. Analysis of the variation of these phonons with increased Ge deposition reveals that step bunching must occur during the initial stages of growth. Raman strain shifts within the 20-ML thick Ge epilayer grown in the presence of a surfactant reveals that areas of strain must co-exist with regions of relaxed Ge, which is also predicted by a growth model involving step bunching.

## II. EXPERIMENT

The experiments were carried out in an ultrahigh vacuum (UHV) chamber with a base pressure of  $5 \times 10^{-10}$  mbar. The samples were either *singular* Si(001) (Unisil, *n*-type, phosphorus,  $1 - 10\ \Omega\ \text{cm}$ ), or *vicinal* Si(001) (VSI, *p*-type, boron,  $> 10\ \Omega\ \text{cm}$ ) cut  $4^\circ$  off the [001] direction towards [110].

The Si samples were cleaned through heating by passing a direct current through them. Care was taken when cleaning the *vicinal* samples that the direction of current flow was parallel to the step edges so as to avoid current induced step migration effects. After an overnight degas at  $600^\circ\text{C}$ , the samples were cleaned by stepwise heating to  $950^\circ\text{C}$ , making sure that the vacuum chamber pressure did not exceed  $2 \times 10^{-9}$  mbar. Sample temperatures were measured by optical pyrometry. When the samples had cooled down to room temperature after cleaning, the *singular* samples produced a double-domain ( $1 \times 2$ ) low-energy electron diffraction (LEED) pattern while the *vicinal* samples showed a significant single-domain character, with a 3:1 domain ratio for ( $1 \times 2$ ):( $2 \times 1$ ), obtained by measuring LEED half order spot intensities.

Once clean, the samples were subjected to two different experiments: Ge growth on clean surfaces and on surfaces terminated with a monolayer of Sb. In all experiments, the Si(001) substrates were heated to  $400^\circ\text{C}$  and Ge were evaporated from a miniature Knudsen cell (K-cell) evaporator. The substrate growth temperature was chosen in order to avoid desorption of the Sb prelayer during growth, while maintaining a high enough temperature to promote ordering of the Ge overlayer. The K-cell had been previously calibrated by means of reflectance anisotropy spectroscopy (RAS), where the reflected signal during the initial growth of Ge on a clean *vicinal* Si(001) sample was known to oscillate with monolayer sensitivity.<sup>24</sup> This method for coverage determination meant that the estimated error in Ge coverage was less than 10%. In preparation for surfactant growth, 4 MLs of Sb were deposited onto clean Si(001) at room temperature. The surface was then annealed at  $450^\circ\text{C}$  for 10 min. Annealing causes the excess Sb to desorb leaving behind an Sb monolayer terminated Si(001) surface with a ( $2 \times 1$ ) LEED pattern. The chamber geometry allowed the SE signal to be monitored during growth. The ellipsometer used in this work is described elsewhere.<sup>22</sup>

The Raman experiments were carried out using nearly identical preparation conditions to those used for the SE work. In contrast to the SE work, the chamber geometry meant that RS measurements could not be recorded during Ge growth. Growth was interrupted at several stages and the samples allowed to cool to room temperature before data acquisition. The 514.5 nm (50 mW) and 476.5 nm (20 mW) lines of an argon-ion laser were used as sources for the Raman experiments. The RS spectrometer used in this work has been described elsewhere.<sup>25</sup> All the RS experiments were carried out with the incident and scattered polarization vectors,  $e_i$  and  $e_s$ , respectively, aligned either  $\parallel$  or  $\perp$  to the principal [110] or  $[\bar{1}10]$  axes of the (001) surface.

For the Raman experiments, *vicinal* Si(001) samples cut  $4^\circ$  off the [001] direction towards [110], rather than *singular* Si(001) samples were used. On-axis samples are known to contain approximately equal numbers of two domains separated by single-atomic-height or *S* steps. These domains consist of dimers which differ only by a  $90^\circ$  rotation in dimer orientation. The use of *vicinal* samples stabilizes the formation of a surface containing regular double-atomic height or *D* steps causing an imbalance in domain numbers, thus yielding more dimers oriented in one direction than the other. *Vicinal* samples therefore allow the extraction of extra information concerning dimer orientation, as shall be seen through the analysis of our Raman data.

## III. RESULTS AND DISCUSSION

### A. Spectroscopic ellipsometry

Figure 1 shows changes in the imaginary part of the pseudodielectric function ( $\langle \epsilon_2 \rangle$ ) of Si, derived from the SE raw data during the growth of Ge on a clean *singular* Si(001) sample held at  $400^\circ\text{C}$  with and without the use of an Sb surfactant prelayer. Although the ellipsometer is capable of operating to 1.5 eV, in this figure we show the dielectric function between 3.0 and 4.5 eV only due to problems arising in the detector from stray light produced by glow from the sample heater filament. In both Figs. 1(a) and (b), a decrease in the  $E_2$  (4.25 eV) gap intensity relative to  $E_1$  (3.45 eV) is observed which is expected due to the growth of any overlayer, in this case the Ge overlayer. However, the behavior of  $E_1$  and  $E_2$  can be seen to differ strongly depending on whether the surfactant layer is used or not prior to Ge growth.

In Fig. 1(a), the evolution of  $\langle \epsilon_2 \rangle$  is shown for increased Ge coverage on the ( $2 \times 1$ )-Sb surface. A gradual change in  $\langle \epsilon_2 \rangle$  is observed even upon initial deposition of Ge. These changes show first of all that SE is sensitive to changes in the thickness of the Ge layer on the ML growth scale. An increase in the intensity of  $E_1$  is observed at low energies while at higher energies, a decrease in  $E_2$  is observed [see arrows in Fig. 1(a)]. Figure 1(b) shows the evolution of  $\langle \epsilon_2 \rangle$  during Ge growth onto the bare clean Si(001)-( $1 \times 2$ ) surface. In the absence of the Sb surfactant layer, Ge growth produces similar changes of the  $\langle \epsilon_2 \rangle$  features as those obtained when using the surfactant layer, up to a coverage of 5 MLs [see arrows (1) in Fig. 1(b)]. However, above this thickness, the behavior differs and a large decrease in the amplitude of the  $E_1$  and  $E_2$  peaks is observed [see arrows (2)].

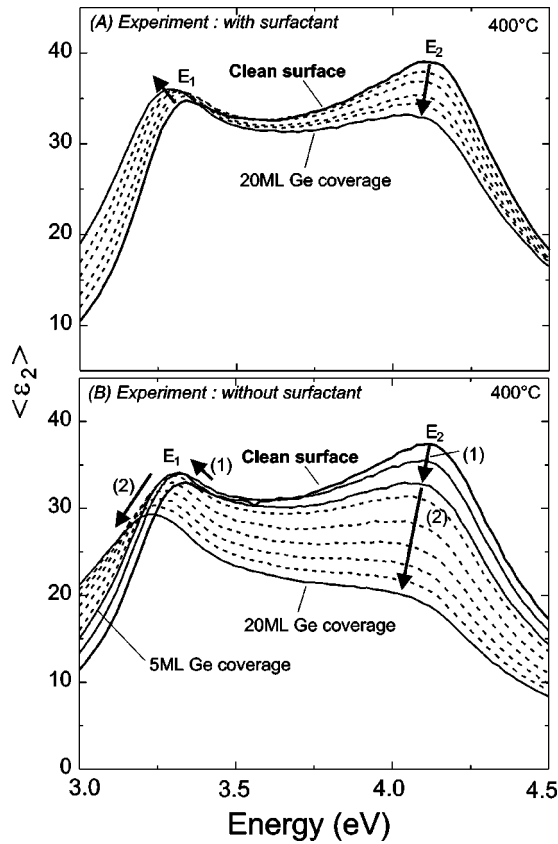


FIG. 1. Plot of the imaginary part of the pseudodielectric function of Si,  $\langle \epsilon_2 \rangle$ , derived from SE data for the growth of Ge on *singular* Si(001) held at 400 °C (A) with, and (B) without an Sb surfactant layer. The arrows indicate changes related to increased Ge growth. In (B) and in the region of the  $E_1$  gap peak at 3.25 eV, (1) refers to an increase of  $\langle \epsilon_2 \rangle$  with initial Ge coverage, while (2) follows the subsequent decrease in  $\langle \epsilon_2 \rangle$  above a critical Ge thickness.

Here, a roughening of the Ge layer is likely to cause this decrease in SE intensity. For a 20-ML-thick Ge layer grown directly onto Si(001), such roughness is known to occur due to the formation of islands and misfit dislocations which alleviate strain caused by the lattice mismatch between both materials.<sup>6,7,9</sup> In the region of the  $E_2$  gap, a larger decrease in intensity is observed in comparison to when a Sb surfactant is used. This is also consistent with the presence of a smooth Ge layer when a surfactant is used and a considerably rough layer when it is not.

In order to analyze the origin of the SE data, we have simulated the SE response using the three layer system (Si substrate/Ge layer/vacuum). In the simulation, the presence of a surfactant is ignored and room-temperature dielectric function data for Si and Ge are used.<sup>26</sup> The well-known Bruggeman effective medium approximation (EMA) was employed to account for roughening effects.<sup>22</sup> This approximation considers rough layers to consist of the sum of a dielectric function for voids, i.e., the empty space between islands, and a dielectric function for the deposited material under investigation.

The results of the simulation are shown in Fig. 2. A shift in peak position is observed by comparing the  $\langle \epsilon_2 \rangle$  experimental and simulated values. This arises from the experi-

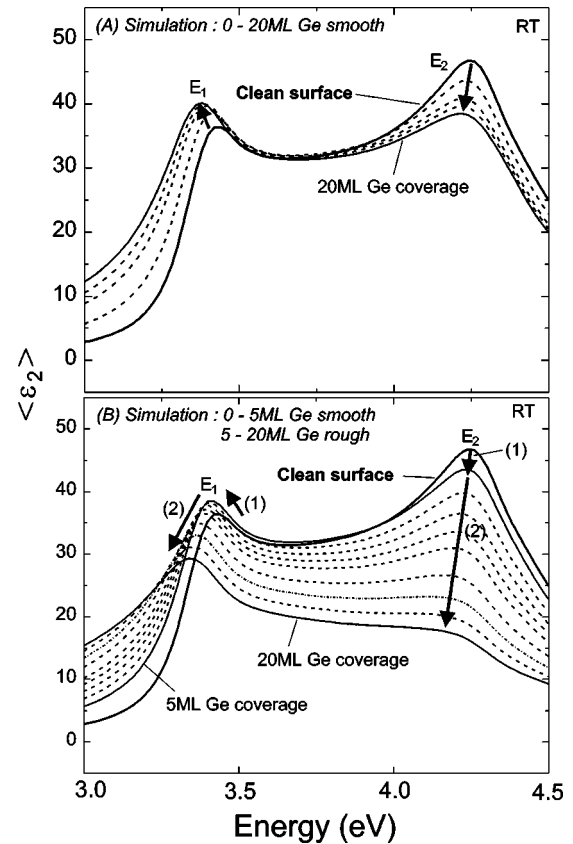


FIG. 2. Plot of simulated  $\langle \epsilon_2 \rangle$  values for the growth of Sb on *singular* Si(001) using room-temperature dielectric function values for Ge and Si (see Ref. 26), (A) assuming the Ge layer grows in a layer-by-layer mode up to 20-MLs imitating the effect of a surfactant and (B) assuming the Ge layer grows in a Stranski-Krastanov growth mode. The arrows indicate changes related to increased Ge growth. In (B), the first five Ge layers are assumed to grow in a layer-by-layer fashion producing the variation labeled (1). Above this coverage, modelling is achieved by considering each layer to consist of a combination of 75% voids and 25% Ge imitating the effect of island growth and producing the variation labeled by (2).

mental data being gathered with the sample at 400 °C rather than at room temperature. By assuming a homogeneous layer 5 MLs thick and subsequent layers to consist of 25% Ge (islands) and 75% voids, the experimental behavior can be reproduced. Initially, an increase in the  $E_1$  gap peak intensity is obtained as a function of Ge layer thickness, followed by a decrease above a thickness of 5 MLs. This is evidence that the SE data shown in Fig. 1 does reveal changes in growth mode, i.e., from layer-by-layer to island growth. Also shown in the figure is a simulation of what is expected if the layer could be forced to remain homogeneous up to a coverage of 20 MLs [see Fig. 2(b)]. Here, a strong similarity to the experimental curve, obtained in the presence of a surfactant layer, is found. This similarity suggests that under our experimental conditions, SE predicts layer-by-layer growth of Ge on Si(001) to be possible at least up to a coverage of 20 MLs. It should be noted, however, that these simulations are based on macroscopic dielectric function data alone, and so microscopic information concerning the quality of the grown layer (i.e., layer defects such as misfit dislocations) cannot be inferred.

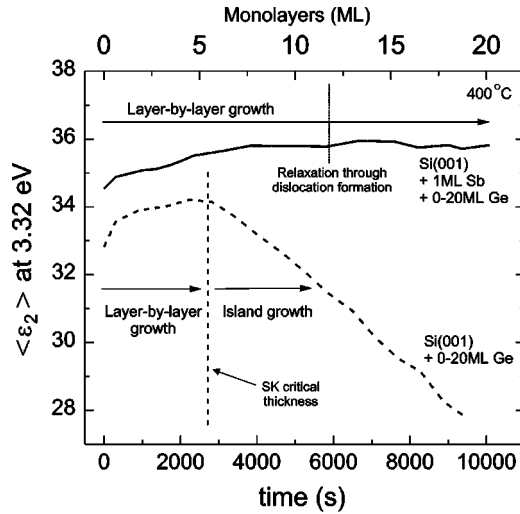


FIG. 3. Plot of  $\langle \epsilon_2 \rangle$  recorded at 3.32 eV.

To see the effect of defects such as dislocations on the SE response, we refer to Fig. 3, which is extracted from the data in Figs. 1 and 2. The figure displays how the SE intensity changes as a function of coverage near the  $E_1$  gap at 3.32 eV. Here, it can be seen that in the presence of a surfactant (solid curve), the critical thickness for dislocations to form and relaxation to occur is well known to take place at a coverage of 11–12 MLs under similar preparation conditions to the ones employed here.<sup>4,10,11</sup> However, despite such relaxation, no change in the SE response is observed. This shows that, despite the ability of SE to determine changes in growth mode, it is insensitive in providing information concerning changes related to strain relaxation, and hence it cannot be used to determine information concerning Ge epilayer quality. As shall be seen in the next section, RS as a surface optical probe shows more potential in this respect.

Finally in the absence of a surfactant, the dashed curve in Fig. 3 clearly shows that above 5 MLs, there is a sharp reduction in intensity when a surfactant layer is not used. As the difference in peak intensity here is directly related to the use of a surfactant, we conclude that the 5-MLs critical thickness must be related to the Stranski-Krastanov (SK) critical thickness where islands are formed, in agreement with the results of previous authors.<sup>6,7,9</sup> However, whether the formation of misfit dislocations accompany this island formation is open to question, as we have shown above that SE is insensitive to defects of this kind.

### B. Raman spectroscopy

In this section, we apply Raman spectroscopy to SMG on a  $4^\circ$  off-cut *vicinal* Si(001) surface. Although surfactant growth has been widely investigated on the *singular* Si(001) surface, and is well understood, no significant experimental study for such growth on the *vicinal* Si(001) surface yet exists. Since the surface energetics of a predominantly single domain *vicinal* Si(001) surface are finely balanced between step repulsion and terrace strain unlike the *singular* Si(001) surface, it is possible that SMG may occur through a different mechanism than that of the *singular* surface.

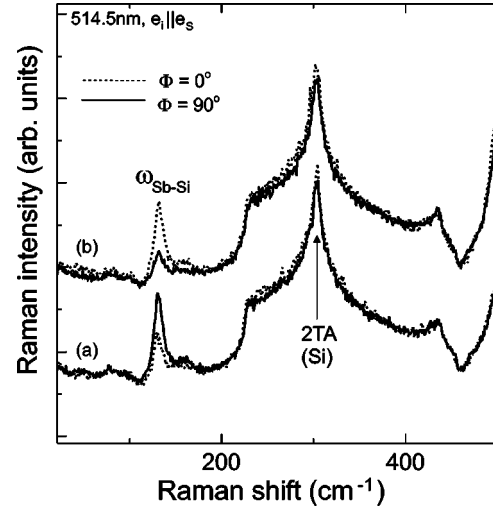


FIG. 4. Raman spectra of the  $(2 \times 1)$ -Sb structure formed on a clean  $4^\circ$  offcut Si(001)- $(1 \times 2)$  sample. The Sb-Sb dimer bond lies along the  $[110]$  direction. Two parallel polarization combinations were used, i.e.,  $e_i \parallel e_s \parallel [110]$  and  $e_i \parallel e_s \parallel [\bar{1}10]$ . Two sample azimuths were used,  $\Phi = 0^\circ$  (a) and  $\Phi = 90^\circ$  (b), effectively reversing both parallel polarization vectors with respect to the sample principal axes. The sample was cooled down to room temperature before data acquisition. The spectra were normalized to the intensity of the LO phonon of bulk Si.

#### 1. Sb monolayer terminated vicinal Si(001)

When 4 MLs of Sb is placed on a clean  $4^\circ$  offcut *vicinal* Si(001) surface, and the sample is subsequently annealed to  $450^\circ\text{C}$ , the excess Sb is desorbed leaving behind the monolayer terminated  $(2 \times 1)$ -Sb structure. Analysis of the Sb induced  $(2 \times 1)$  LEED pattern showed that Sb dimerization had occurred in a direction perpendicular to the underlying Si dimers, that is along  $[110]$ , in agreement with other work.<sup>27</sup> It should be noted that care must be taken in preparing this surface as recent results have indicated that the reconstruction quality is critically dependent on preparation conditions.<sup>28</sup>

Raman data showing the development of a surface phonon peak at  $130.5\text{ cm}^{-1}$  associated with the  $(2 \times 1)$ -Sb structure through these stages of growth was reported by Esser *et al.*<sup>29</sup> Here, we show Raman spectra for the  $(2 \times 1)$ -Sb surface with the polarization vector of the incident and analyzed light,  $e_i$  and  $e_s$ , respectively, oriented along the surface  $[110]$  direction ( $e_i \parallel e_s \parallel [110]$ , solid line), that is parallel to the Sb dimer bond or along the  $[\bar{1}10]$  direction ( $e_i \parallel e_s \parallel [\bar{1}10]$ , dotted line), which is perpendicular to the Sb dimer bond [see Fig. 4(a)]. We define the sample azimuth here to be  $\Phi = 0^\circ$ . From these spectra, we can see that a larger intensity for the Sb related phonon at  $130.5\text{ cm}^{-1}$  is obtained when the polarization vectors are aligned along the Sb-Sb dimer bond direction. Sb adsorption at surface steps can be ruled out as the origin of this peak through comparison of the Sb dimer terminated reconstruction formed on *singular* Si(001).<sup>29</sup> If this peak was due to Sb induced reconstruction at rebonded  $D$ -step edges known to be present at such a vicinal offcut angle,<sup>30</sup> then it would not be expected for the singular surface, which contains no  $D$  steps. However, this peak is observed on the singular surface

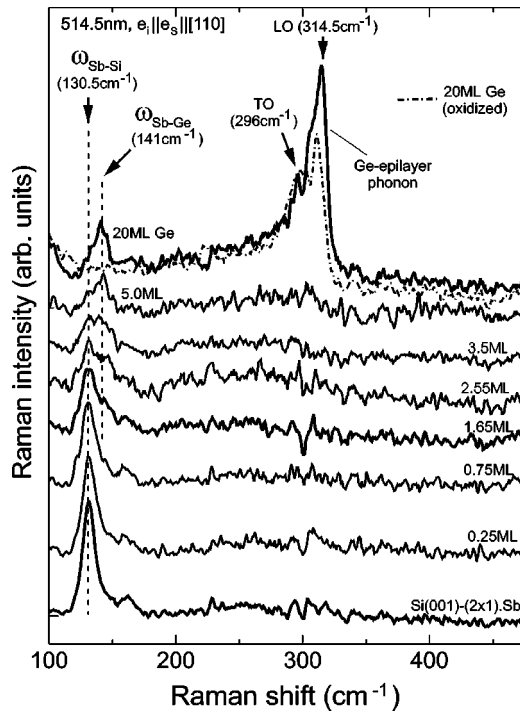


FIG. 5. Raman difference plot (Ge/Sb covered surfaces—clean Si(001) surface) using a 514.5 nm excitation wavelength, taken at stages during the growth of up to 20 MLs of Ge on the *vicinal* Si(001)-(2×1)-Sb surface. The Ge growth was interrupted at the coverages indicated and the sample was cooled down to room temperature before data acquisition. The coverages shown are cumulative and the parallel polarization combination  $e_i||e_s||[110]$  was used where the polarization vectors are initially parallel to the Sb-Sb dimer bond of the (2×1)-Sb surface.

and hence must originate from the Sb-dimer induced terrace structure.<sup>29</sup>

To further investigate the Raman intensity dependence with polarization direction, we rotate the sample azimuthally by 90° ( $\Phi=90^\circ$ ) keeping everything else constant. The results are shown in the spectra labeled (b) in Fig. 4. Now the solid line represents  $e_i||e_s||[\bar{1}10]$  and the dashed line,  $e_i||e_s||[110]$ . The intensity variation of the 130.5 cm<sup>-1</sup> feature switches indicating the intensity must be related to the orientation of the Sb-Sb dimers in the majority domain. We label this surface phonon mode as  $\omega_{Sb-Si}$ . The sensitivity of RS to surface domain occupancies demonstrates its potential as a surface characterization probe. As this feature is only observed when the parallel polarization combination, that is when  $e_i||e_s$  is oriented along either of the principal [110] or  $[\bar{1}10]$  axes only, it has been identified as an  $A_1$  eigenmode which defines a symmetric vibration in the plane normal to the surface and parallel to the Sb-Sb dimer bond.<sup>29</sup>

## 2. Surface phonons: Establishing a growth model for SMG on vicinal Si(001)

Ge was then deposited on the (2×1)-Sb terminated *vicinal* surface held at 400 °C. Figure 5 shows the Raman spectra taken using the polarization combination,  $e_i||e_s||[110]$ , and the coverage where the growth was interrupted is indicated in the figure. The spectra shown are difference spectra, and signify subtraction of the clean Si(001)-(1×2) from the

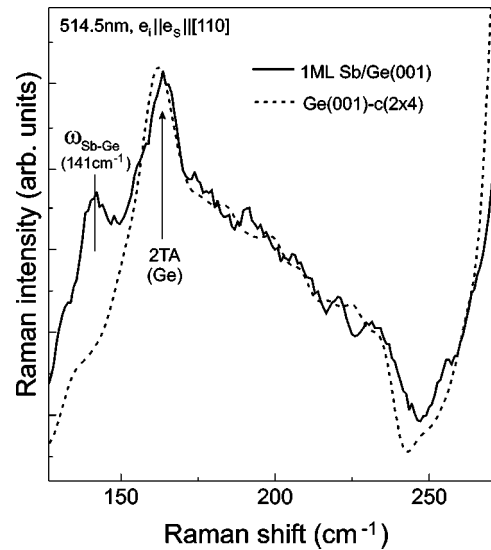


FIG. 6. Raman spectra, using a 514.5 nm excitation wavelength, of the Ge(001) surface after growth of a 10 ML Ge buffer layer and after the growth of 1 ML of Sb on this surface. The parallel polarization combination,  $e_i||e_s||[110]$  was used. The sample was cooled down to room temperature before data acquisition. The spectra were normalized to the LO phonon of bulk Ge.

covered surface spectrum. This allows clear observation of the Ge-Ge phonon mode which occurs at approximately 300 cm<sup>-1</sup> over the second-order bulk Si transverse acoustical (2TA) phonon which dominates the Raman spectrum in the 300-cm<sup>-1</sup> spectral region (see Fig. 4).

From Fig. 5 it can be seen that the  $\omega_{Sb-Si}$  surface phonon mode at 130.5 cm<sup>-1</sup> reduces gradually in intensity during growth and has disappeared above a Ge coverage of 3.5 MLs. Another phonon peak becomes apparent at a Ge coverage exceeding 2.55 MLs at the slightly higher energy of 141 cm<sup>-1</sup>. The origin of the peak at 141 cm<sup>-1</sup> was identified through a separate experiment by depositing Sb on a singular Ge(001) sample. The Ge(001) surface was cleaned by thermal annealing to 700 °C followed by deposition of a 10 ML Ge buffer layer. Under these conditions, a weak  $c(2\times 4)$  LEED pattern was observed. Once clean, 1 ML of Sb was deposited on this surface. The Raman results are shown in Fig. 6, again for the  $e_i||e_s||[110]$  configuration. From the figure, a feature centred at 141 cm<sup>-1</sup> is clearly visible. Like the  $\omega_{Sb-Si}$  surface phonon, no feature was observed for the crossed polarization combination, i.e.,  $e_i\perp e_s$  (not shown in Fig. 6). Through similar selection rule arguments as used for  $\omega_{Sb-Si}$ , we associate the feature at 141 cm<sup>-1</sup> with a surface phonon mode involving Sb dimers bonded to the Ge(001) surface. This indicates that the feature we observe at 141 cm<sup>-1</sup> after growth of 20 MLs of Ge mediated by Sb must be related to Sb bonding on the Ge epilayer. Supporting evidence for an Sb dimer termination of a Ge epilayer grown on Si(001) comes from previous scanning tunneling microscopy (STM) work.<sup>31,32</sup> Hence the feature at 141 cm<sup>-1</sup> is likely to involve Sb dimers bonded to the underlying Ge layer. We label this phonon as  $\omega_{Sb-Ge}$ . In Fig. 6, the Raman spectrum for Ge also reveals a feature at 162 cm<sup>-1</sup> which is the second-order transverse acoustic (2TA) phonon peak of Ge. The bulk 2TA peak is approximately 20 times smaller in amplitude than the Ge bulk LO

phonon (not shown in Fig. 6). Hence the 2TA feature cannot be observed in the Raman spectrum for the Ge epilayer (see Fig. 5), as a peak 20 times smaller than the Ge epilayer LO phonon would place this 2TA phonon in the noise level of our experiment.

Further evidence that the  $\omega_{Sb-Ge}$  phonon at  $141\text{ cm}^{-1}$  is a surface feature comes from its removal after the Sb/20-ML-Ge/Si(001) sample was deliberately oxidized through exposure to air (see Fig. 5). Exposing the sample to air is a well-known way to determine whether a feature observed under UHV conditions is indeed a surface feature, as exposure to air generally destroys any surface features through surface reactions involving oxygen. The  $\omega_{Sb-Ge}$  phonon is removed through exposure to air, confirming that it was a surface feature. It should be noted that despite the existence of many Raman studies of this system,<sup>33–37</sup> this data represent an observation of surface related phonons involving Sb at  $130.5\text{ cm}^{-1}$  (for  $\omega_{Sb-Si}$ ) (see also Ref. 29) and  $141\text{ cm}^{-1}$  (for  $\omega_{Sb-Ge}$ ). All previous Raman studies have been carried out in air, after the surfactant had been removed and a thick Si layer grown to protect the Ge layer.<sup>33–37</sup>

By following the intensity of the  $\omega_{Sb-Si}$  and  $\omega_{Sb-Ge}$  surface phonons with Ge coverage, interesting information concerning SMG on *vicinal* Si(001) is revealed (see Fig. 5). First, a gradual reduction in the  $\omega_{Sb-Si}$  peak intensity at  $130.5\text{ cm}^{-1}$  with increasing Ge coverage up to 3.5 MLs is observed indicating a gradual loss of Sb dimers from the interface. This is in conflict with the general understanding of SMG where no thermodynamic or kinetic barrier to Sb site exchange is expected upon deposition of above 0.5 MLs of Ge, especially for growth at an elevated temperature of  $400\text{ }^\circ\text{C}$ .<sup>17,18</sup> From such a growth model, we would expect to see complete removal of the  $\omega_{Sb-Si}$  surface phonon by deposition of between 0.5–1.0 MLs and not the gradual reduction in intensity that we observe up to deposition of 3.5 MLs of Ge.

We propose that the only reasonable model that can successfully explain the gradual disappearance of this phonon and the appearance of the  $\omega_{Sb-Ge}$  phonon must be related to changes in step structure at the initial stages of Ge growth. Any layer-by-layer growth model cannot satisfactorily explain the intensity dependence upon Ge coverage observed of both surface phonons. For example, if a 2D Ge layer were hypothetically allowed to cover the Sb layer above 0.5-ML coverage, then a shift in phonon frequency for the  $\omega_{Sb-Si}$  phonon would be inevitable. Since no shift is observed, such a model is impossible.

In order to understand the mechanism of growth occurring here, it is important to first explain briefly the nature of steps on a  $4^\circ$  clean vicinal Si(001) surface. On such a surface, a regular array of steps of double atomic height (*D* steps) rather than single atomic height (*S* steps) are stabilized. The formation of a significant amount of *D* steps occurs for samples with vicinal offcuts greater than  $2^\circ$  in order to reduce the step repulsion term, which dominates the surface energetics when steps become too close.<sup>38</sup> When *D* steps are formed, the terrace width must double in order to maintain the vicinal angle. Hence the formation of *D* steps halves the number of steps on the surface, and because the terrace width has doubled, the step repulsion energy is reduced.

Although the step repulsion term controls the surface energetics, the surface is still under considerable stress due to dimerization of Si atoms on the terraces. Now, if this surface is exposed to an additional stress, elastic relaxation around each step causes a long-range attractive interaction between them, leading to step bunching, which is independent of whether an external flux is present or on the initial step density of the sample.<sup>39</sup> In our work, the additional stress is provided by the size difference between the growing Ge and the Si substrate. Hence, initially, as surfactant exchange is completed and Ge bonds with the Si substrate, the steps become increasingly bunched. Such bunching has been observed experimentally for Ge growth on a bare  $3.9^\circ$  offcut Si(001) surface.<sup>13</sup> STM revealed bunched *D*-type steps, separated by  $20\text{ \AA}$  terraces, along with wider terraces  $200\text{ \AA}$  in width.<sup>13</sup> Although step bunching on the bare vicinal surface was not observed until the sample annealing temperature exceeded  $600\text{ }^\circ\text{C}$ ,<sup>13</sup> in the presence of Sb, which is also known to affect the step structure of a vicinal Si(001) sample,<sup>40</sup> the temperature for step bunching may be substantially reduced.

We propose that step bunching occurs during deposition of the first Ge ML or so. This also implies the generation of wide terraces in order to preserve the overall  $4^\circ$  vicinal angle [see Fig. 7(b)]. As these wide terraces now constitute much of the surface area, surfactant mediated layer-by-layer growth commences here preferentially through the well understood mechanism for surfactant exchange outlined by Copel and co-workers<sup>2,3</sup> [see Fig. 7(b)]. As the diffusion of impinging Ge is known to be limited by Sb on these broad terraces, they grow at the expense of the narrow step-bunched regions. As well as Ge impinging directly on these terraces, they are also supplied indirectly with Ge which diffuses over the bunched step regions. From the theoretical work of Oh *et al.*,<sup>19</sup> Sb bonding at *D* steps causes a reduction in its associated Schwoebel barrier, allowing Ge to diffuse over the step edges, and presumably, to become incorporated at the lowest step of the step bunch. Hence the terraces of the step bunched regions are starved of Ge and so, Sb dimers can still be found here bound to the bare Si surface at Ge coverages, where on the *singular* surface, such bonding would have long disappeared. This mechanism readily explains why the  $\omega_{Sb-Si}$  surface phonon is observed at coverages above 1 ML [see Fig. 7(b)].

According to the work of Tersoff and co-workers, in the presence of a flux, such as Ge, step bunching reaches a maximum and then decreases through step overgrowth.<sup>39</sup> Once step bunching has maximized on our surface, subsequent deposition of layer-by-layer grown Ge causes the steps to be gradually overgrown. With the appearance of more Ge at the step-bunched region, SMG is promoted and hence the  $\omega_{Sb-Si}$  surface phonon feature gradually disappears while the  $\omega_{Sb-Ge}$  feature appears [see Fig. 7(c)]. Since the  $\omega_{Sb-Si}$  surface phonon disappears above 3.5 MLs of Ge deposition, this coverage is related to the coverage where all bunched steps have been overgrown (see Fig. 5). At the same time, the  $\omega_{Sb-Ge}$  phonon is further established, consistent with the exchange of Sb to the surface of the Ge epilayer. Subsequent growth is expected to occur in a layer-by-layer fashion [see Fig. 7(d)]. It is worth noting that an interface comprising bunched steps will give rise to fluctuations in layer thickness

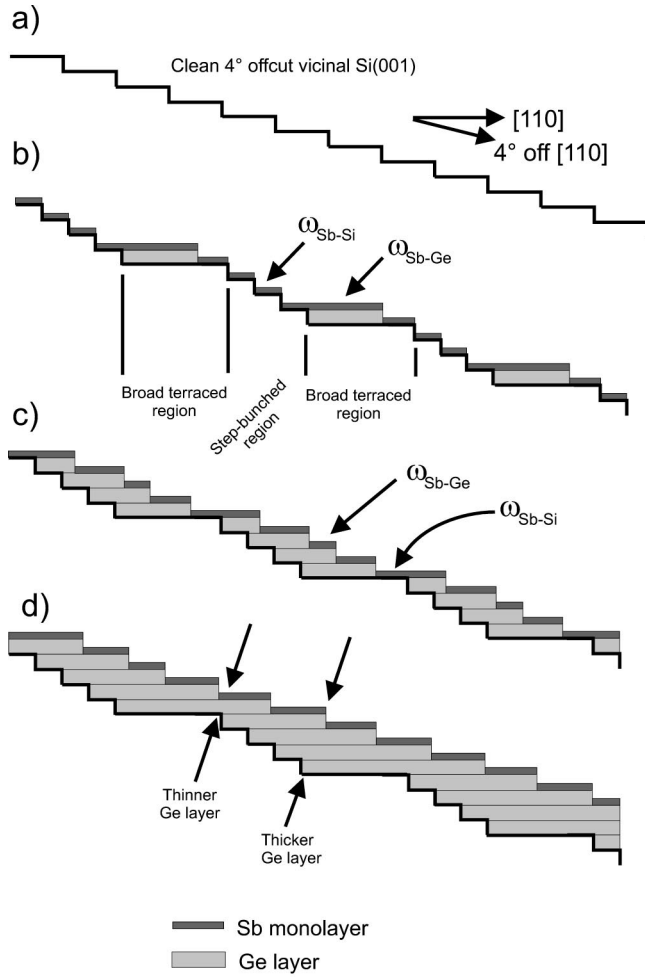


FIG. 7. Model for the initial stages of SMG on vicinal Si(001). (a) shows the step structure of an ideal 4° offcut Si(001) sample. In (b), the extra stress induced by the lattice mismatch between Sb, Ge, and the vicinal Si(001) substrate leads to step bunching as outlined in Refs. 13 and 14. SMG takes place predominantly on the broad terraces. In (c), the step bunched regions have nearly been overgrown with Ge and surfactant exchange of Sb is largely complete. In (d), the substrate steps have been overgrown and the Ge epilayer thickness has increased. It can be seen that substrate step bunching leads to inhomogeneities in Ge thickness which in turn lead to inhomogeneities in strain.

once the growth is terminated [see Fig. 7(d)]. We return to this point in the next section.

In the spectroscopic ellipsometry section, we discussed SE data for SMG on *singular* Si(001). From the discussion above, it would appear that SE, which we have shown to be sensitive to the growth mode for such a system, would be appropriate in determining whether step bunching does indeed occur during the initial stages of SMG on *vicinal* Si(001). However, the differences between a surface containing a regular array of steps, or less but bunched steps, would be small since the average surface roughness would not be much affected. Thus it follows that the difference in an SE spectrum caused by step bunching would be negligible.

### 3. Ge epilayer phonon: The determination of Ge epilayer quality

Upon observation of Fig. 5, along with the surface phonon peaks, a strong asymmetric and broad feature, previ-

ously related to a Ge-Ge vibration<sup>33–37</sup> is observed in the region of 314.5 cm<sup>-1</sup>, but only for a Ge coverage of 20 MLs. This peak is shifted relative to the bulk Ge-Ge vibration which is known to occur at approximately 300 cm<sup>-1</sup> and can be explained in terms of strain within the 20 ML Ge epilayer. Analysis of this strain gives us information concerning the quality of the 20 ML-grown Ge epilayer. For 5 ML Ge coverage, a small broad feature just above the noise level of our experiment is observed in the region of 250–300 cm<sup>-1</sup> (see Fig. 5). Observation of this peak at lower Ge coverages was not possible owing to poor sensitivity of the Raman experiment in separating the Ge signal from the strong 2TA contribution of the Si bulk.

The effect of strain within any pseudomorphic epilayer grown on a Si(001) substrate on the LO phonon associated with that layer is to remove its degeneracy, producing a doublet consisting of frequency shifted LO and TO branches. The effect of strain in Raman spectroscopy was treated in detail by Anastassakis<sup>41</sup> and others.<sup>42,43</sup> The strain induced shift of the LO and TO phonon frequencies can be approximated by<sup>43</sup>

$$\Delta\omega_{LO} = -\omega_0\epsilon_L, \quad (1)$$

$$\Delta\omega_{TO} = \frac{1}{2}\omega_0\epsilon_L, \quad (2)$$

where  $\omega_0$  is the phonon frequency of an unstrained layer, while

$$\epsilon_L = \frac{a_{Si} - a_{Ge}}{a_{Ge}}. \quad (3)$$

We note that  $\epsilon_L < 0$  for a compressively strained epilayer, where  $a_{Si}$  and  $a_{Ge}$  correspond to the lattice constant of the substrate and epilayer, respectively. Assuming a 4.2% lattice mismatch between Ge and Si and the unstrained Ge-Ge vibration frequency to be 300 cm<sup>-1</sup> (see Ref. 33), we expect the LO phonon frequency to be shifted up in energy by approximately 12.6 cm<sup>-1</sup> and the TO frequency to be shifted downwards by 6.3 cm<sup>-1</sup>. From examination of Fig. 5, we observe that the Ge-Ge feature consists of two significant contributions centered at 314.5 and 296 cm<sup>-1</sup>, respectively, causing shifts of 14.5 and 4 cm<sup>-1</sup>, respectively, with respect to the unstrained bulk Ge-Ge value. These shifts agree well with the calculated shifts thus confirming that the Ge epilayer grown in the presence of a surfactant still contains regions under strong compressive strain. We assign the features to the epilayer Ge-Ge LO and TO phonons, respectively. Small discrepancies between the experimental and calculated shift demonstrate that some relaxation has occurred within these strained regions. From Fig. 5 it can also be seen that after oxidation, the Ge-Ge LO and TO phonons are still resolvable at 310.8 and 297 cm<sup>-1</sup>, respectively, indicating that strain still exists, although some convergence towards the degenerate bulk LO value has occurred indicating further relaxation.

Despite the main contributions to the Ge-Ge phonon peak being the strained LO and TO doublet, the overall broadness of the Ge epilayer phonon peak shown in Fig. 5 indicates that the layer, although still containing some strained regions indicative of a layer-by-layer grown epilayer, is by no means

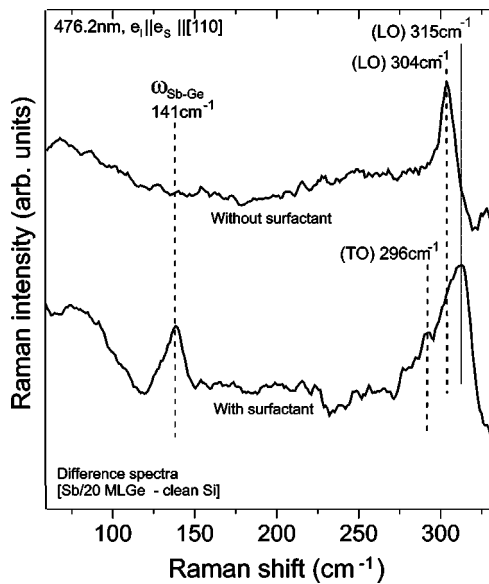


FIG. 8. Raman spectra, using a 476.2 nm excitation wavelength, showing the frequency of the Ge-Ge vibration after the deposition of a nominal Ge thickness of 20 MLs with and without the use of Sb as a surfactant. The sample was cooled down to room temperature before data acquisition.

perfect. In Fig. 8, we compare the Ge-Ge peaks obtained in the presence and absence of the surfactant layer using the 476.2 nm line of the Ar ion laser. First, it is clear from the figure that the presence of Sb greatly affects the shape of the Ge-Ge related feature. Without the surfactant, a sharper Ge peak is observed centered at  $304 \text{ cm}^{-1}$ . This indicates that without the surfactant, the Ge layer has undergone substantial relaxation, which is well known to occur through the formation of misfit dislocations.<sup>4,10,11</sup> For growth of Ge in the presence of the Sb surfactant, the Ge epilayer LO peak at  $315 \text{ cm}^{-1}$  contains a significant shoulder at  $304 \text{ cm}^{-1}$ . Observation of this shoulder clearly demonstrates relaxation within the Ge epilayer (see Fig. 8). A background asymmetric broadening of the Ge-Ge Raman feature towards lower energies is also present suggesting that disorder due to thickness variations are also present within the Ge layer. This is consistent with the growth model outlined in the last section, where inhomogeneities in Ge thickness are expected to exist due to growth on a step bunched Si(001) substrate [see Fig. 7(d)]; hence the thin regions produce a strain shifted LO and TO phonon contribution, being closer to the 11–12 ML critical thickness for dislocation formation, while the thicker regions are more likely to be relaxed and defect.

No distinct Ge-Ge feature is observed in the region of  $300\text{--}320 \text{ cm}^{-1}$  for a Ge coverage of 5 MLs despite its ob-

servation by other authors at this coverage.<sup>33–37</sup> Previous work has either been carried out at different excitation energies, polarization combinations, or growth conditions. The work of Tsang *et al.*,<sup>36</sup> for example, showed a significant peak in the region of  $300\text{--}310 \text{ cm}^{-1}$  even for 2–3 ML-Ge coverage but the excitation wavelength used was 568 nm or 2.18 eV, which is close to the  $E_1$  resonance of bulk Ge. Two previous studies have been carried out using 514.5 nm excitation, one by Osten *et al.*,<sup>33</sup> who observed a small Ge-Ge peak at 4 ML-Ge coverage but for a cross polarization combination. Ichimura *et al.*<sup>37</sup> also used a 514.5 nm excitation and found a small peak in the region of  $300\text{--}310 \text{ cm}^{-1}$  for a 7 ML-Ge covered sample, which, along with being of greater thickness than our 5 ML thickness, the polarization combination used was not quoted and so direct comparison with our results is not possible.

#### IV. CONCLUSIONS

In this paper we have shown that spectroscopic ellipsometry (SE) and in particular, Raman spectroscopy (RS), can provide information concerning SMG of Ge on *singular* and *vicinal* Si(001). In the absence of a surfactant and at low Ge coverages, SE shows that an SK growth mode exists on the *singular* Si(001) surface and that the critical thickness for island formation is in the region of 5 MLs, in agreement with other work. Using RS, two surface optical phonons have been found for SMG on *vicinal* Si(001); one associated with Sb-Sb dimers bonded to Si ( $130.5 \text{ cm}^{-1}$ ) and the other with Sb-Sb dimers bonded to Ge ( $141 \text{ cm}^{-1}$ ) opening up new possibilities for the understanding of surfactant processes. The behavior of these phonons during the initial stages of Ge growth is explained by step bunching, which is driven by the strain associated with the lattice mismatch between Sb and Ge, and the *vicinal* Si(001) substrate. Under the growth conditions used, and in the presence of a Sb monolayer deposited prior to Ge growth, RS also shows evidence of strain and relaxation within a 20 ML thick Ge epilayer, pointing to inhomogeneities within the epilayer. Such inhomogeneities can be explained as a direct consequence of step bunching.

In general, the aim of this paper has been to elucidate the power of surface optics in deducing key parameters of the complex processes involved in surfactant mediated growth. It is hoped that the potential of surface optics outlined here will lead to more experimental investigations in this direction.

#### ACKNOWLEDGMENTS

J. R. Power acknowledges support from the Alexander Von Humboldt foundation.

\*Present address: Infineon Technologies, TDL, Königsbrücker Strasse 180, Dresden, D01099, Germany.

†Present address: Institut für Spektrochemie und angewandte Spektroskopie (ISAS), Albert Einstein Strasse 9, Berlin-Adlershof, D-12489, Germany.

<sup>1</sup>R.D. Bringans, R.I.G. Uhrberg, M.A. Olmstead, and R.Z. Bachtch, *Phys. Rev. B* **34**, 7447 (1986).

<sup>2</sup>M. Copel, M.C. Reuter, E. Kaxiras, and R.M. Tromp, *Phys. Rev.*

*Lett.* **63**, 632 (1989).

<sup>3</sup>M. Copel, M.C. Reuter, M. Horn-von Hoegen, and R.M. Tromp, *Phys. Rev. B* **42**, 11 682 (1990).

<sup>4</sup>A.A. Williams, J.M.C. Thornton, J.E. MacDonald, R.G. van Silfhout, J.F. van der Veen, M.S. Finney, A.D. Johnson, and C. Norris, *Phys. Rev. B* **43**, 5001 (1991).

<sup>5</sup>M. Diani, D. Aubel, J.L. Bischoff, L. Kubler, and D. Bolmont, *Surf. Sci.* **291**, 110 (1993).



- <sup>6</sup>D.J. Eaglesham and M. Cerullo, Phys. Rev. Lett. **64**, 1943 (1990).
- <sup>7</sup>Y.-W. Mo, D.E. Savage, B.S. Swartzentruber, and M.G. Lagally, Phys. Rev. Lett. **65**, 1020 (1990).
- <sup>8</sup>F.K. LeGoues, M. Copel, and R.M. Tromp, Phys. Rev. B **42**, 11 690 (1990).
- <sup>9</sup>I. Goldfarb, P.T. Hayden, J.H.G. Owen, and G.A.D. Briggs, Phys. Rev. Lett. **78**, 3959 (1997).
- <sup>10</sup>J.M.C. Thornton, A.A. Williams, J.E. MacDonald, R.G. van Silfout, M.S. Finney, and C. Norris, Surf. Sci. **273**, 1 (1992).
- <sup>11</sup>M. Horn-von Hoegen, B.H. Miller, and A. Al-Falou, Phys. Rev. B **50**, 11 640 (1994).
- <sup>12</sup>F. Wu, X. Chen, Z. Zhang, and M.G. Lagally, Phys. Rev. Lett. **74**, 574 (1995).
- <sup>13</sup>L.W. Guo, N. Lin, Q. Huang, J.M. Zhou, and N. Cue, Appl. Surf. Sci. **126**, 213 (1998).
- <sup>14</sup>J.-H. Zhu, K. Brunner, and G. Abstreiter, Appl. Phys. Lett. **73**, 620 (1998).
- <sup>15</sup>R.M. Tromp and M.C. Reuter, Phys. Rev. Lett. **68**, 954 (1992).
- <sup>16</sup>B.D. Yu and A. Oshiyama, Phys. Rev. Lett. **72**, 3190 (1994).
- <sup>17</sup>M.A. Boshart, A.A. Bailes III, and L.E. Seiberling, Phys. Rev. Lett. **77**, 1087 (1996).
- <sup>18</sup>M. Jiang, X.-Y. Zhou, B.-X. Li, and P.-L. Cao, Phys. Rev. B **60**, 8171 (1999).
- <sup>19</sup>C.W. Oh, E. Kim, and Y.H. Lee, Phys. Rev. Lett. **76**, 776 (1996).
- <sup>20</sup>*Optical Characterization of Epitaxial Semiconductor Layers*, edited by G. Bauer and W. Richter (Springer-Verlag, Berlin, Heidelberg, 1996).
- <sup>21</sup>N. Esser and W. Richter, *Light Scattering in Solids, VIII*, edited by M. Cardona and G. Güntherodt (Springer-Verlag, Berlin, Heidelberg, 2000), Vol. 76, p. 96.
- <sup>22</sup>U. Rossow and W. Richter, *Optical Characterisation of Epitaxial Semiconductor Layers*, edited by G. Bauer and W. Richter (Springer-Verlag, Berlin, Heidelberg, 1996), Chap. 3.
- <sup>23</sup>D.E. Aspnes, Thin Solid Films **89**, 249 (1982).
- <sup>24</sup>J.R. Power, P. Weightman, S. Bose, A.I. Shkrebtii, and R. Del Sole, Surf. Sci. **433-435**, 373 (1999).
- <sup>25</sup>N. Esser, Appl. Phys. A: Mater. Sci. Process. **69**, 507 (1999).
- <sup>26</sup>D.E. Aspnes and A.A. Studna, Phys. Rev. B **27**, 985 (1983).
- <sup>27</sup>M. Richter, J.C. Woicik, J. Nogami, P. Pianetta, K.E. Miyano, A.A. Baski, T. Kendelewicz, C.E. Bouldin, W.E. Spicer, C.F. Quate, and I. Lindau, Phys. Rev. Lett. **65**, 3417 (1990).
- <sup>28</sup>Y.J. Lee, J.W. Kim, and S. Kim, J. Phys.: Condens. Matter **9**, L583 (1997).
- <sup>29</sup>N. Esser, K. Hinrichs, W. Richter, and J. R. Power, Surf. Sci. (to be published).
- <sup>30</sup>D.J. Chadi, Phys. Rev. Lett. **59**, 1691 (1987).
- <sup>31</sup>U. Köhler, O. Jusko, B. Miller, M. Horn-von Hoegen, and M. Pook, Ultramicroscopy **42-44**, 832 (1992).
- <sup>32</sup>O. Jusko, U. Köhler, G.J. Pietsch, B. Miller, and M. Henzler, Appl. Phys. A: Solids Surf. **54**, 265 (1992).
- <sup>33</sup>H.J. Osten, E. Bugiel, B. Dietrich, and W. Kissinger, Appl. Phys. Lett. **64**, 1723 (1994).
- <sup>34</sup>R.L. Headrick, J.-M. Baribeau, D.J. Lockwood, T.E. Jackman, and M.J. Bedzyk, Appl. Phys. Lett. **62**, 687 (1993).
- <sup>35</sup>S.S. Iyer, J.C. Tsang, M.W. Copel, P.R. Pukite, and R.M. Tromp, Appl. Phys. Lett. **54**, 219 (1989).
- <sup>36</sup>J.C. Tsang, S.S. Iyer, and S.L. Delage, Appl. Phys. Lett. **51**, 1732 (1987).
- <sup>37</sup>M. Ichimura, A. Usami, A. Wakahara, and A. Sasaki, J. Appl. Phys. **77**, 5144 (1995).
- <sup>38</sup>E. Pehlke and J. Tersoff, Phys. Rev. Lett. **67**, 465 (1991).
- <sup>39</sup>J. Tersoff, Y.H. Phang, Z. Zhang, and M.G. Lagally, Phys. Rev. Lett. **75**, 2730 (1995).
- <sup>40</sup>J. Wasserfall and W. Ranke, Surf. Sci. **331-333**, 1099 (1995).
- <sup>41</sup>E. Anastassakis, J. Appl. Phys. **68**, 4561 (1990).
- <sup>42</sup>*Numerical Data and Functional Relationships in Science and Technology*, Landolt-Bornstein, New Series, Group III, Vol. 17, Pt. a, edited by O. Madelung (Springer, Berlin, 1983).
- <sup>43</sup>N. Esser and J. Geurts *Optical Characterisation of Epitaxial Semiconductor Layers* (Ref. 20), Chap. 4.